MATERIALS CHARACTERIZATION 62 (2011) 706–715

available at www.sciencedirect.com

ScienceDirect

www.elsevier.com/locate/matchar

Analysis of atomic force microscopy data for surface characterization using fuzzy logic

Amjed Al-Mousa[a], *Darrell L. Niemann*[a], *Devin J. Niemann*[b], *Norman G. Gunther*[a], *Mahmud Rahman*[a,*]

[a]*Electron Devices Lab., Electrical Engineering Dept., Santa Clara University, Santa Clara, USA*
[b]*University of California- Santa Cruz, Santa Cruz, USA*

ARTICLE DATA

Article history:
Received 10 February 2011
Received in revised form 5 April 2011
Accepted 7 April 2011

Keywords:
Characterization
Nanostructures
Atomic force microscopy
Fuzzy logic

ABSTRACT

In this paper we present a methodology to characterize surface nanostructures of thin films. The methodology identifies and isolates nanostructures using Atomic Force Microscopy (AFM) data and extracts quantitative information, such as their size and shape. The fuzzy logic based methodology relies on a Fuzzy Inference Engine (FIE) to classify the data points as being top, bottom, uphill, or downhill. The resulting data sets are then further processed to extract quantitative information about the nanostructures. In the present work we introduce a mechanism which can consistently distinguish crowded surfaces from those with sparsely distributed structures and present an omni-directional search technique to improve the structural recognition accuracy. In order to demonstrate the effectiveness of our approach we present a case study which uses our approach to quantitatively identify particle sizes of two specimens each with a unique gold nanoparticle size distribution.

1. Introduction

The surface topology of electronically active films can significantly influence the characteristics of the devices in which they are incorporated [1,2]. Therefore, advanced surface characterization techniques are becoming increasingly important for effective design and performance modeling of such devices. Conventional characterization methods focus on computing statistical metrics of the entire surface such as RMS, surface roughness, average height, etc. [3,4]. These methods typically lack the ability to identify surface features of individual structures. Thresholding is also a very common analysis technique where a user sets a cut-off value such that any data value below the threshold is deemed to be part of the surface floor, while any data above the threshold is deemed to be part of a structure. A clustering algorithm is then applied to group neighboring structure points into one structure [5]. The main issue with thresholding is the definition of the threshold, an inappropriate choice can result in biased results. A more complex analysis technique, called Watershed [6,7], works very well for sparse surfaces. However, when it comes to dense crowded surfaces it results in over-segmentation artifacts.

Previously, we have presented and applied a new systematic analysis technique to characterize surface topology information derived from Atomic Force Microscopy (AFM) data [8–10]. This technique is based on isolating surface nanostructures and extracting quantitative information such as their shape and size. Our methodology is independent of feature size, and does not require a data-dependent threshold. Furthermore, our technique can readily be extended to operate on other types of Scanning Probe Microscopy (SPM) data.

* *Corresponding author at:* Electron Devices Laboratory, Dept. of Electrical Engineering, Santa Clara University, 500 El Camino Real, Santa Clara, CA 95053, USA. Tel.: +1 408 554 4175; fax: +1 408 554 5474.
E-mail addresses: aalmousa@vt.edu (A. Al-Mousa), guntherng@msn.com (N.G. Gunther), mrahman@scu.edu (M. Rahman).

1044-5803/$ – see front matter © 2011 Elsevier Inc. All rights reserved.
doi:10.1016/j.matchar.2011.04.001

In this work we introduce a mechanism which can consistently distinguish crowded surfaces from those with sparsely distributed structures. The entire mechanism is completely automated. Detecting the surface type is an essential step that will help tune the Fuzzy Inference Engine (FIE) parameters to yield the best results. In addition, we present an omni-directional search technique to improve the association of each surface point with its corresponding structure. Using this technique, each surface point searches a 360° planar range to find the appropriate structure to be associated with. In previous implementations this process was limited to two orthogonal directions. The new grid-independent technique enables structure detection with enhanced precision.

We also present a case study where our technique is used to quantitatively identify the particle size distributions for two specimens consisting of gold nanoparticles dispersed on a mica surface. Each of the two specimens has a different particle count, different nominal particle size, and particle size distribution. The results presented have been obtained by implementing the technique using MATLAB 7.5.0 (R2007b) and the Fuzzy Logic toolbox version 2.2.6.

1.1. *Terminology*

Our methodology will be described in terms of specific terminology as illustrated in Fig. 1 which shows a 3D visualization of a small segment of an AFM data set representing solid particles of different sizes. Here, we define the terms height, top, the bottom and the gradient x/y as indicated in the figure.

A structure is identified by a collection of neighboring data points, which we refer to as Structure Points (SPs). Each structure point is characterized by the unique coordinates (x, y) and the height of the surface at that point. This information is used to compute the gradient along the horizontal direction (G_x) and the gradient along the vertical direction(G_y) for each SP. Fig. 2 shows 13 SPs which can be grouped into three structures (AA, BB and CC). We compute the structure size by tracking the number of SPs contained in a given structure. In addition we compute the structure envelope, which is the area of the smallest rectangle the encompassed all SPs in a given structure. Table 1 shows both of the size and envelope computed for all three structures in Fig. 2.

2. Fuzzy Logic Technique

In order to eliminate the need for data-dependent filtering and other arbitrary intervention we have developed an alternate approach that employs a Mamdani fuzzy logic system to classify the surface points [11]. The Fuzzy logic approach carries with it the advantage of being inherently insensitive to anomalous data and has been applied to problems of similar nature [12,13]. The fuzzy logic based approach analyses the AFM data in three steps, as illustrated in Fig. 3.

The first step of the technique is to detect the surface type, which is detailed in Section 2.1. Next in Section 2.2, the Point Classification step is examined, where each point of the surface is classified as a top, bottom, uphill, or downhill. In the Top Clustering step, Section 2.3, neighbouring tops are grouped to form the nucleus of a structure. At the last step, the association process is completed by linking uphill and downhill points to their appropriate top in Section 2.4.

2.1. *Surface Type Detection*

In this section we introduce a mechanism which distinguishes crowded surfaces from those with sparsely distributed structures. The detection of surface type is necessary to enhance the Fuzzy Inference Engine (FIE). This determination serves as a basis for determining the boundaries of the fuzzy input membership functions.

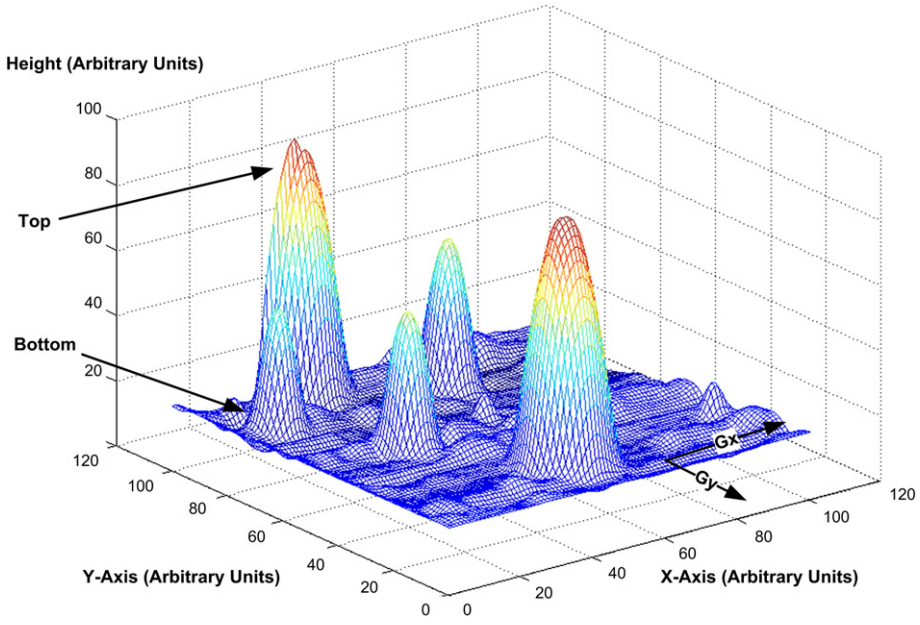

Fig. 1 – A 3D schematic illustration of a portion of a microsurface illustrating the terminology used in this paper.

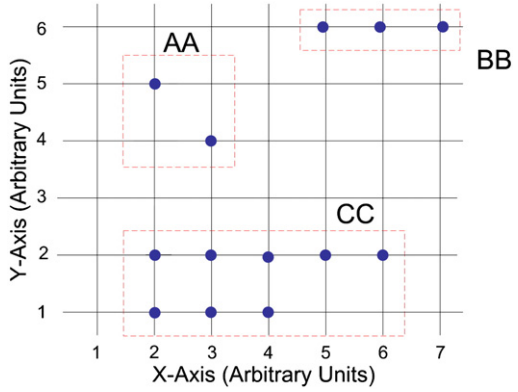

Fig. 2 – A 2D schematic of the surface showing the grouping of neighboring structure points into their respective structures AA, BB, and CC.

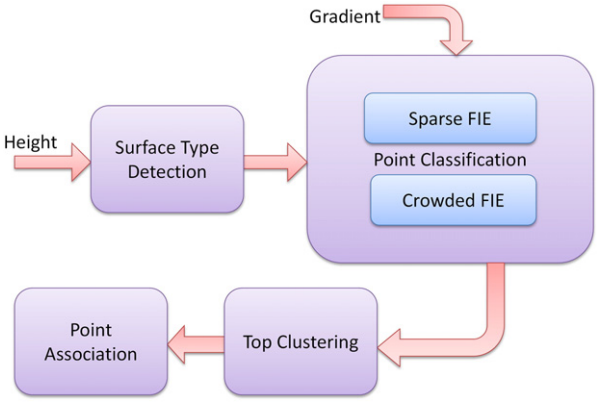

Fig. 3 – Flow chart for the fuzzy logic technique, indicating the four steps which identify structures using height and gradient information.

The detection of the surface type is done by comparing the statistical distribution of the height of the sample points to the range. The statistical parameters used to characterize the height distribution are the first, second, and third quartiles (Q1, Q2 and Q3, respectively). These three parameters divide the height statistical distribution into four subsets each containing a quarter of the distribution. Samples where Q_2 "median" falls closer to the minimum of the range are classified as sparse surfaces. While if Q_2 is at the middle of the range or higher the surface is classified as crowded.

Fig. 4a shows a sparse surface with 3 gold particles on a mica surface. Fig. 4b, on the other hand, shows a crowded surface consisting of pentacene crystals grown on a mica substrate. It is evident from Fig. 5 that the height distribution for the first specimen is concentrated around the lower part of the range, while for the second specimen it is a Gaussian around the middle of the range.

2.2. *Classification Of Surface Points Using A Fuzzy Inference Engine (FIE)*

The inputs to the FIE are the height and the derived gradient information available for each surface point in the data set. The output of the system is a topographical categorization of each surface point, as shown in Fig. 6.

First, the height (H), the gradient in the horizontal direction (G_x), and the gradient in the vertical direction (G_y) are fuzzified. The fuzzification process transforms discrete values measured from the specimen into fuzzy membership functions. For H we have three membership functions, viz., Large, Medium, and Small, as shown in Fig. 7a. Similarly, for G_x and G_y, there are also three membership functions Positive, Negative, and Zero, shown in Fig. 7b. The data are processed by determining a membership for each point into one of these three input classes prior to being passed to the FIE.

As will be shown in Section 3.1, knowing the surface type is essential to yielding the best results. For sparse surfaces, the

Table 1 – Statistics collected for the structures in Fig. 2.

Structure	AA	BB	CC
Size	2	3	8
Envelope	4	3	10

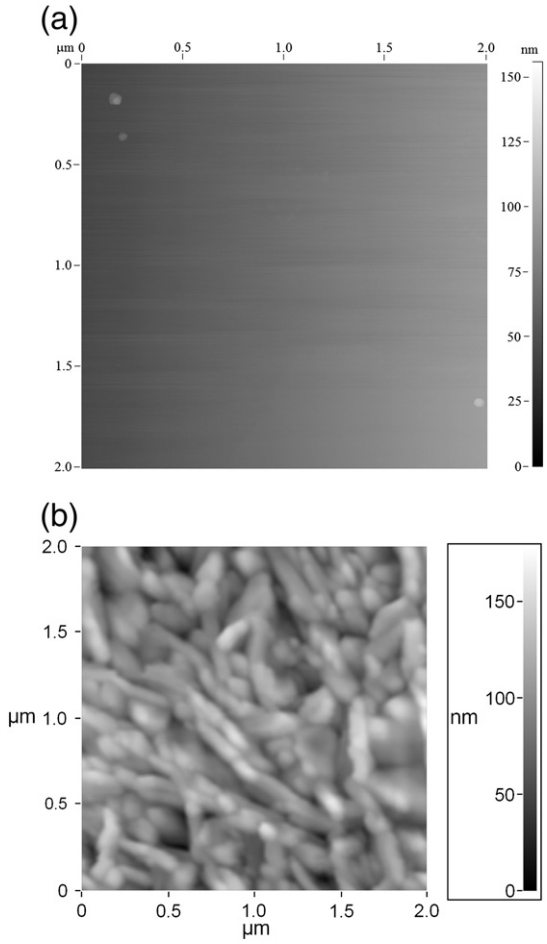

Fig. 4 – (a) Raw AFM data of three gold particles on mica surface (2 μm×2 μm). (b) Raw AFM data of pentacene grown on mica substrate (2 μm×2 μm).

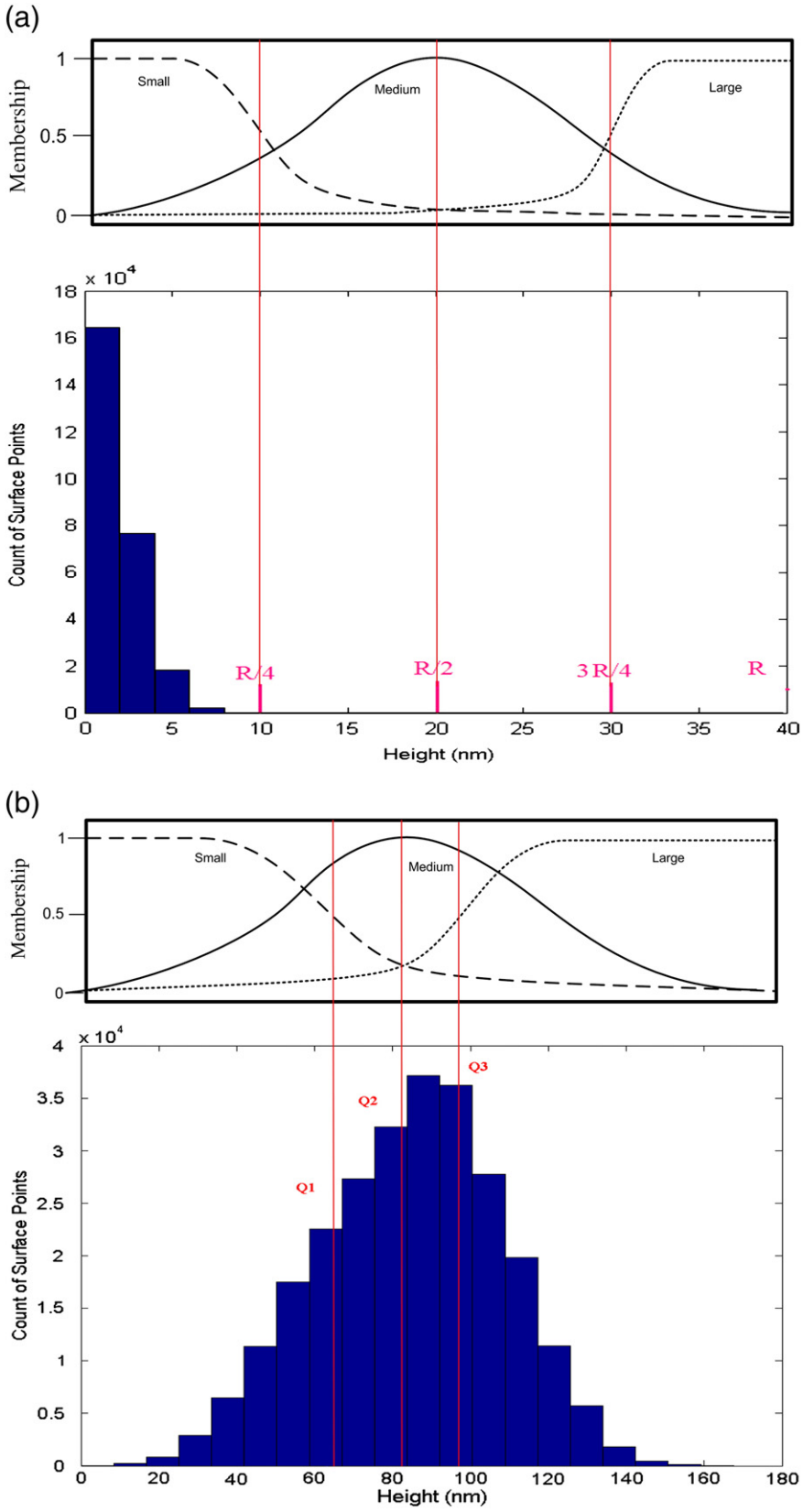

Fig. 5 – (a) Histograms of height data for gold particles of Fig. 4a, where the span of the data is used to define the ranges of the fuzzy membership functions. (b) Histogram of height data for pentacene structures of Fig. 4b. Here the first, second, and third quartiles (Q1, Q2 and Q3) are used to define the ranges of the fuzzy membership functions.

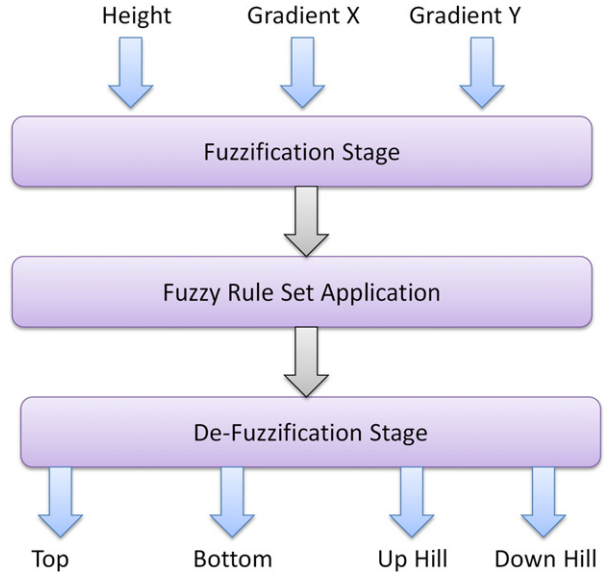

Fig. 6 – Flow diagram for the surface point classification step.

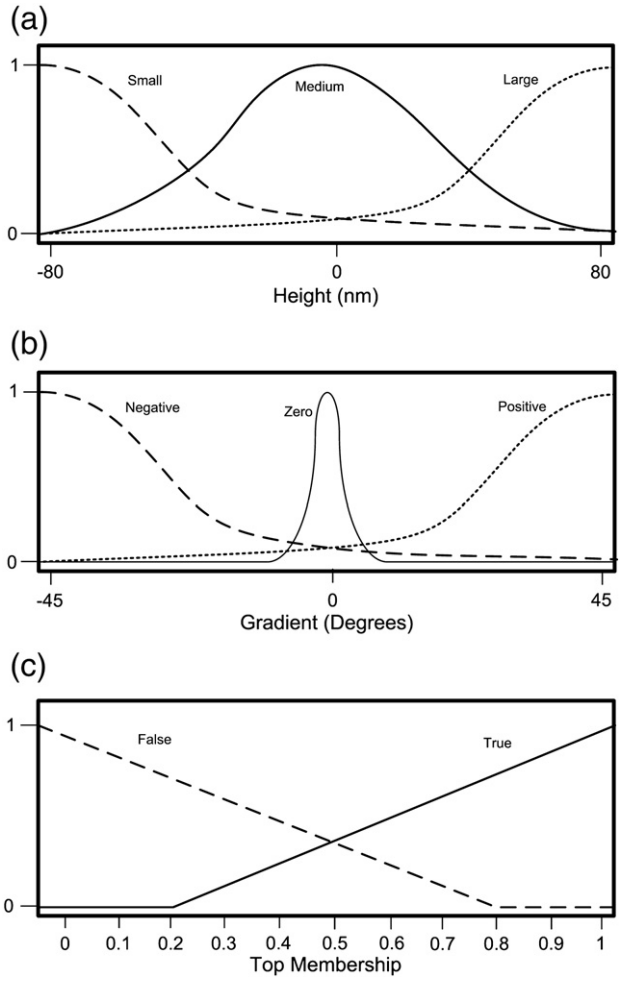

Fig. 7 – (a) Typical height input membership function. (b) Typical gradient input membership function. (c) 'True'–'false' classification scheme for top membership function.

membership functions are distributed uniformly over the entire height range R, as shown in Fig. 5a. For crowded surfaces, on the other hand, the membership functions are distributed using the first, second, and third quartiles (Q_1, Q_2, and Q_3), as shown in Fig. 5b.

The fuzzy rule set, given in Table 2, decides the category of each surface point based on the membership of the current point and its neighbours. This allows each point to be classified as part of either an uphill, downhill, top, or bottom. The result of applying the rules contained in the FIE is a membership ranking of each point in each of the output variables.

These results are aggregated and de-fuzzified using the True-False membership function, shown in Fig. 7c. The de-fuzzification process transforms fuzzy membership functions back into discrete values. The variable with the largest membership ranking will determine the classification of the current point.

2.3. *Clustering Of Tops Of Structures*

The third step in the process is the clustering of the tops of surfaces. Once individual points are classified, the tops of structures are clustered based on their proximity to each other. These clustered tops will form the basis of the final structure. For visualization purposes each structure top is distinguished by a randomly assigned color. Due to artefacts in the measurement and the fuzzy nature of the algorithm, false tops may appear. In the specimens examined below, tops consisting of one or two pixels are deemed to be anomalous because they are close to the noise level of the instrument used thus they are removed.

2.4. *Linking Of Uphill And Downhill Surface Points*

In the previous step the tops of the structures are clustered. Now we are left with points that are classified as bottom, uphill, and downhill points. While the bottom points are not considered to be associated with any structure, the uphill and

Table 2 – Sample table of classification rules for the fuzzy inference engine.

Height\ Gx	Positive	Zero	Negative
Large		Top	
Medium	Up		Down
Small		Bottom	
Height\ Gy	**Positive**	**Zero**	**Negative**
Large		Top	
Medium	Up		Down
Small		Bottom	
Gx\ Gy	**Positive**	**Zero**	**Negative**
Positive	Up	Up	
Zero	Up	Top/bottom	Down
Negative		Down	Down
Height			
Large			Top
Medium			Up/down
Small			Bottom

downhill points must be linked. An omni-directional search technique is deployed to associate each surface point with its corresponding structure. Using this technique, each surface point searches a 360° planar range to find the appropriate structure to associate with. While searching, if a bottom is encountered before reaching a top, then the entire cone angle created by that bottom will be excluded from the search range and thus will not be included in the subsequent processing. In Fig. 8, the top (C) is closer to the current point than top (B). Despite their proximity there is the bottom (A) blocking the top (C), thus, it is not a candidate for association. Consequently, if a point is surrounded by bottoms from all directions, that point will not be connected to any other point.

This is a significant improvement over previous implementations where this process was limited to two orthogonal directions [8]. The omni-directional search enables structure detection with enhanced precision.

Now that the algorithm has identified tops, grouped them together, disregarded bottoms, and linked up and down hills to corresponding tops, a unique identifier can be assigned to each structure. This identifier is used to collect and track statistical information about each structure such as its size, envelope, average height, etc.

3. Results And Technique Testing

3.1. *Sparse Vs. Crowded Surfaces*

Fig. 4 shows examples illustrating the two different types of AFM data sets. Fig. 4a is a mica surface bearing only three scattered gold particles, while Fig. 4b depicts pentacene crystals on a mica substrate. After processing each of these films, the structures are identified and assigned a randomly generated color to distinguish adjacent structures. These results

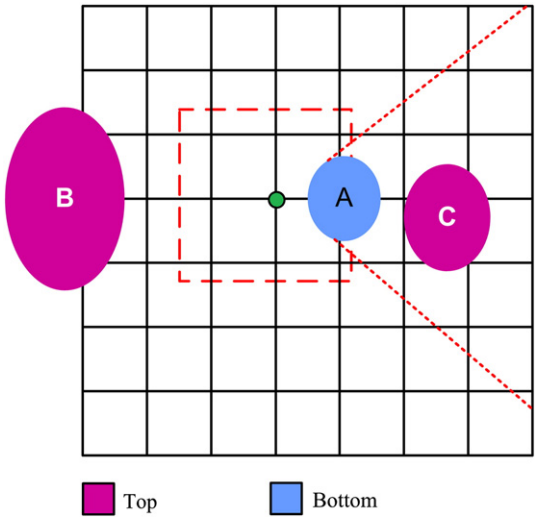

Fig. 8 – Omni-directional searching improves point clustering. Here the current point (green dot) is closer to the 'top' C than to the 'top' B, but it cannot be clustered with it because C is shadowed from it by 'bottom' A.

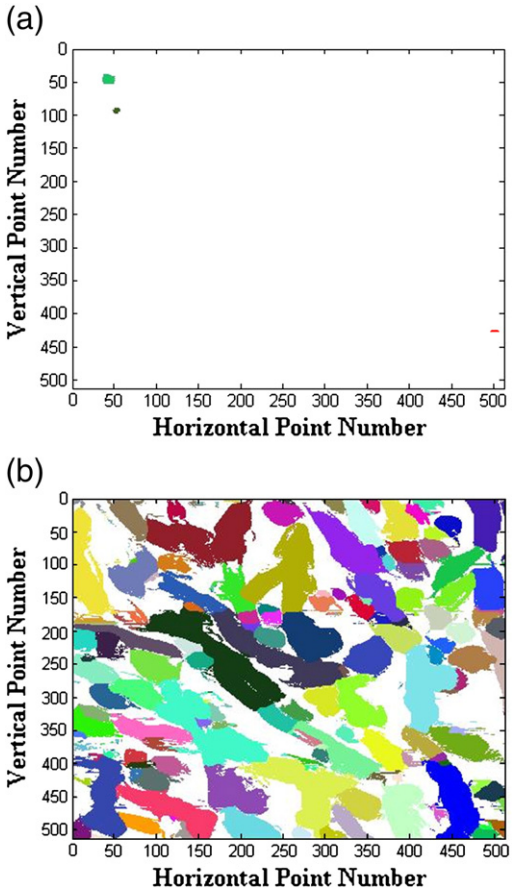

Fig. 9 – (a) The three gold particles shown in Fig. 4a were recognized successfully by our technique. (b) Pentacene surface structures shown in Fig. 4b were also successfully recognized by our technique. Colors are randomly assigned.

are shown in Fig. 9 where we can see that the three distinct particles in Fig. 4a were indeed detected and are clearly visible in Fig. 9a. Meanwhile, for the second specimen we can see the resemblance of the structures detected in Fig. 9b to the original AFM data in Fig. 4b. It is evident that our method has succeeded in recognizing and characterizing the structures without ambiguity.

3.2. *Comparing Gold Particle Specimens*

In this section we present the analysis of a set of experimental data aimed at testing the performance of our technique. Both test cases include well defined nanoparticles of different sizes. The first specimen, shown in Fig. 10a, is 5 μm × 5 μm, and consists of gold particles on mica substrate. These particles have a nominal diameter of 50 nm. The results of analyzing this specimen (Specimen-1) using our technique is shown in Fig. 10b. This data demonstrates that our methodology is able to recognize the particles shown in the original AFM image. The sizes of these individual particles are also estimated based on this analysis. Fig. 10c shows the distribution of the particle sizes recognized using the fuzzy technique.

The next specimen we analyzed (Specimen-2) is also 5 μm × 5 μm. This sample consists of fewer particles and

includes several larger particles. The original AFM data in Fig. 11a indicates roughly two particle sizes large ones in the range of 200 nm and smaller ones below 100 nm. When processing this specimen using our technique the difference in size is readily apparent, as shown in Fig. 11b. The particle size distribution shown in Fig. 11c confirms the existence of two distinct groups of particles: one between 140 and 220 nm and the other between 60–100 nm, which is consistent with the original AFM data.

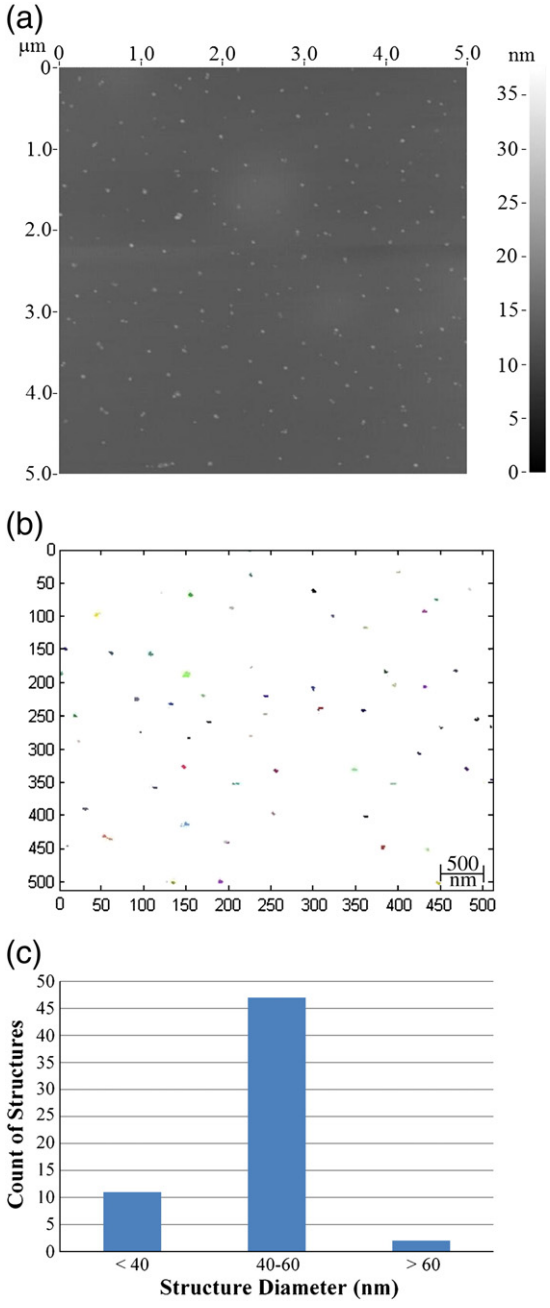

Fig. 10 – (a) Raw AFM data (Specimen-1) of gold particles (50 nm) on mica surface (5 μm × 5 μm). (b) Data shown in Fig. 10a after being processed and successfully recognized by our technique. (c) Histogram of the sizes of the recognized particles shown in Fig. 10b.

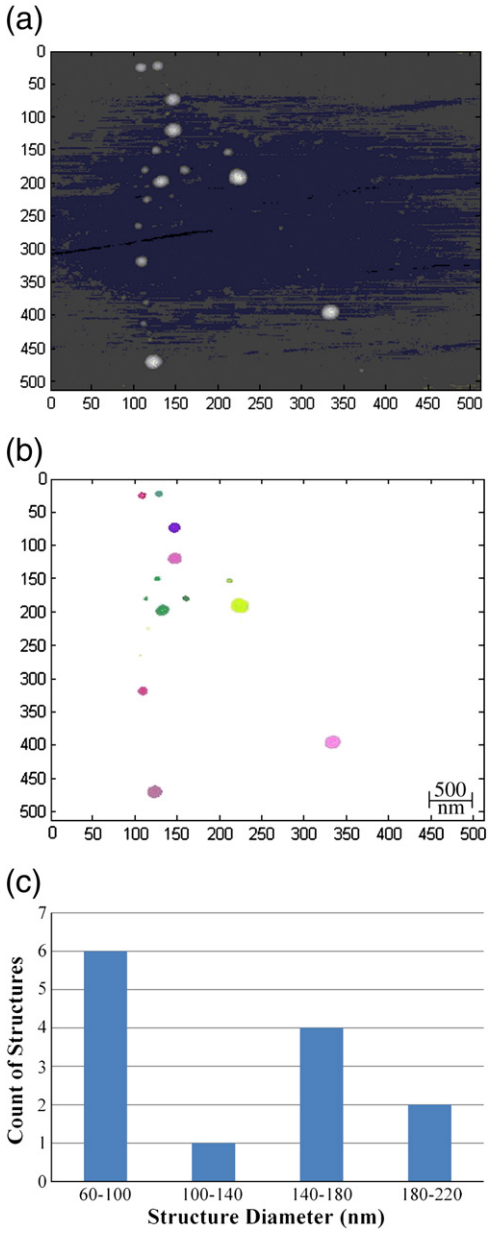

Fig. 11 – (a) Raw AFM data (Specimen-2) of gold particles on mica surface (5 μm × 5 μm). (b) The gold particles shown in Fig. 11a were recognized successfully by our technique. (c) Histogram of the sizes of the recognized particles shown in Fig. 11b.

Since the size of all particles has been measured for Specimen-1 and Specimen-2, the average particle diameter can be estimated for each specimen. These results are shown in Fig. 12, where we can see the average particle size for Specimen-2 is around 130 nm. Meanwhile, Specimen-1 has an average diameter of 47 nm. Thus, this process can be used to analyze and compare multiple films efficiently and accurately. It is interesting to note that while the smaller particle distribution in Fig. 10c is apparently Gaussian, that for the large particles shown in Fig. 11c appears to be bimodal.

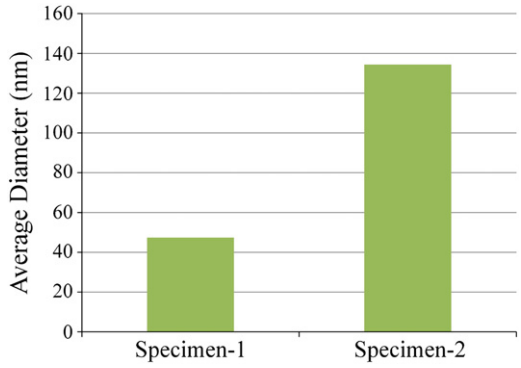

Fig. 12 – Comparison between the particle diameters in Specimen-1 and Specimen-2.

4. Comparison Against Other Techniques

In this section, the results obtained using other analysis techniques are presented. Here, the Thresholding, Watershed, and Edge Detection techniques are used to analyze some of the samples that have been analyzed using the enhanced fuzzy logic.

4.1. *Thresholding Results*

The SPM data visualization and analysis tool, Gwyddion, is used to analyze the mica sample shown in Fig. 10b. In this sample, the maximum height is 160 nm as measured from the lowest point in the sample. A manual calibration is needed to pick the best threshold level. In Fig. 13, the results of applying the thresholding technique are shown using the following levels: 90, 100, 110, and 120 nm.

It can be seen that a 90 nm threshold, shown in Fig. 13a, results in a large number of structures being combined into larger ones. In Fig. 13b, the threshold level of 100 nm shows better results by not combining as many structures as before. However, the boundaries of the recognized structures do not correspond well to the boundaries apparent upon visual inspection of the same image. These two images highlight two key draw backs of using thresholding on crowded surfaces. Fig. 13c shows a 110 nm threshold, this level shows that the recognized structures are smaller than expected and

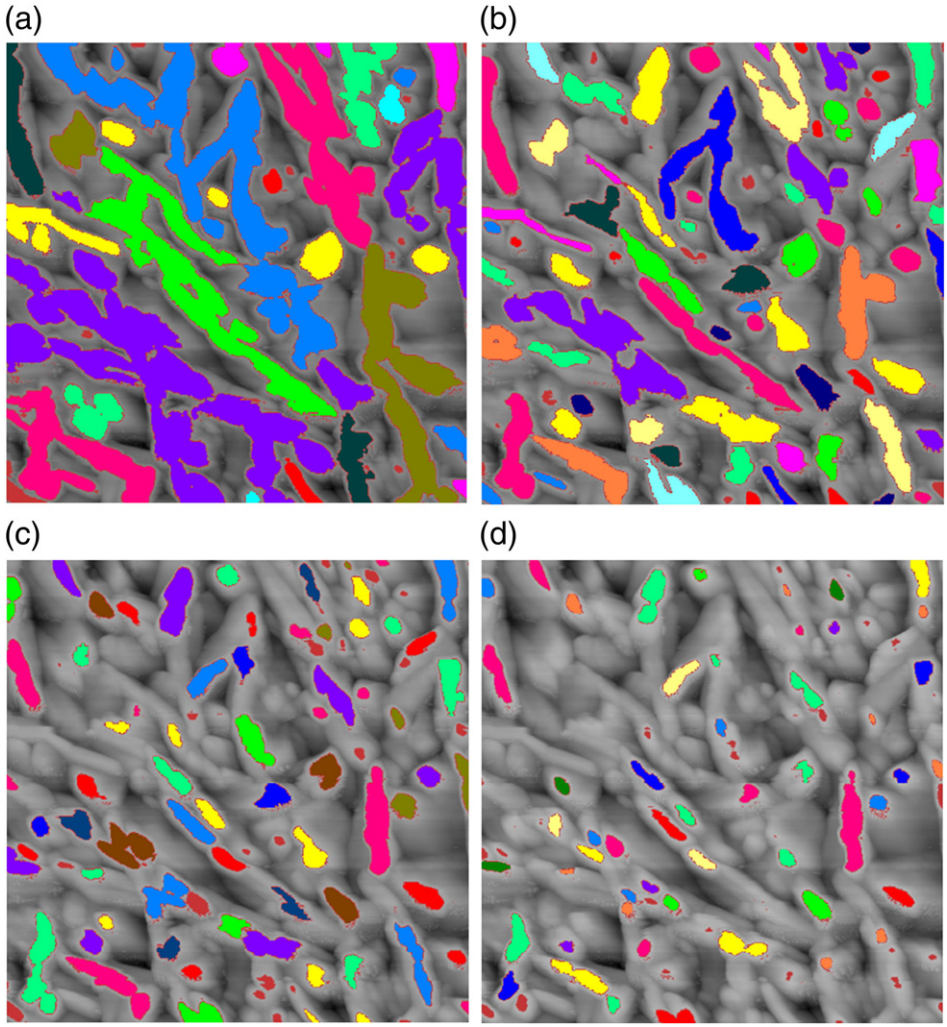

Fig. 13 – Results of applying thresholding technique to pentacene film on mica Sample shown in Fig. 4b. (a) Threshold = 90 nm. (b) Threshold = 100 nm. (c) Threshold = 110 nm. (d) Threshold = 120 nm.

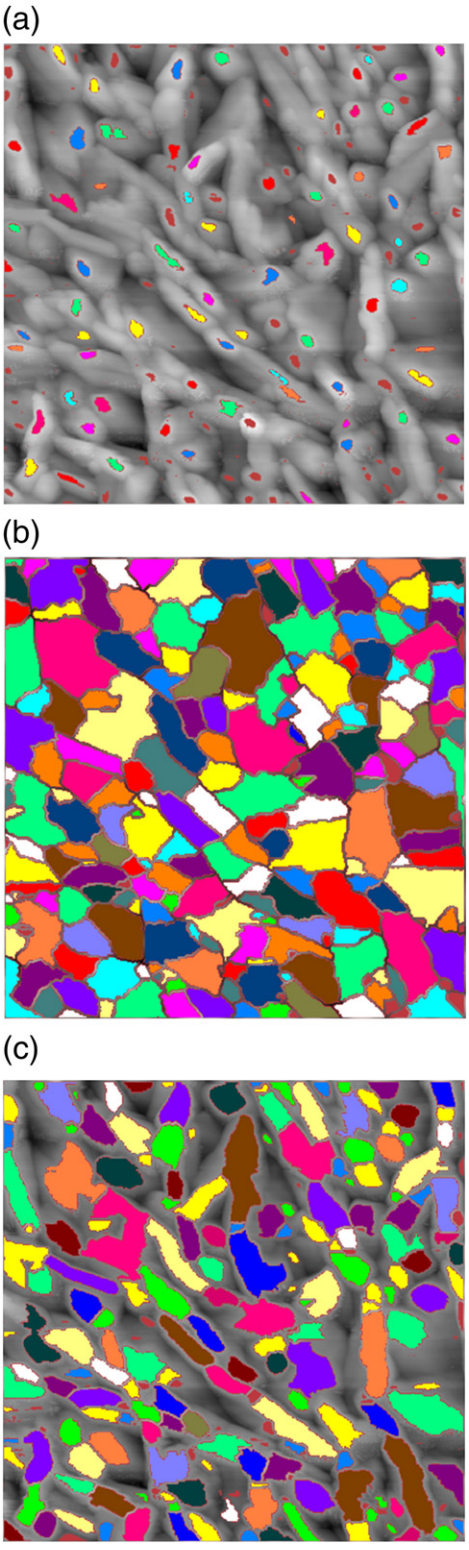

Fig. 14 – Results of applying watershed technique to pentacene film on mica sample shown in Fig. 4b. (a) Default tool settings. (b) Effect of missing bottoms. (c) Best results obtained using watershed.

some of the structures are lost. Finally, Fig. 13d shows how significant parts of the structures are missed due to only a slight increase in the threshold.

The previous results show the complications of choosing the right threshold. It also shows a major deficiency of the thresholding technique in detecting the boundaries of the structures compared to the enhanced fuzzy logic technique.

4.2. *Watershed Results*

The Gwyddion tool has also been used to analyze the pentacene on mica data using the Watershed Technique. Fig. 14a shows the results of analysis using the watershed technique with the default parameters. It is readily apparent that many structures have been missed and that the areas of the detected structures are smaller than the apparent areas in the original data.

With five parameters to tune in the watershed technique, figuring out the right combination to yield the best results is quite a challenge and requires a thorough understanding of the technique. Fig. 14b, shows another combination of the parameters that initially seem to yield improved results. However,

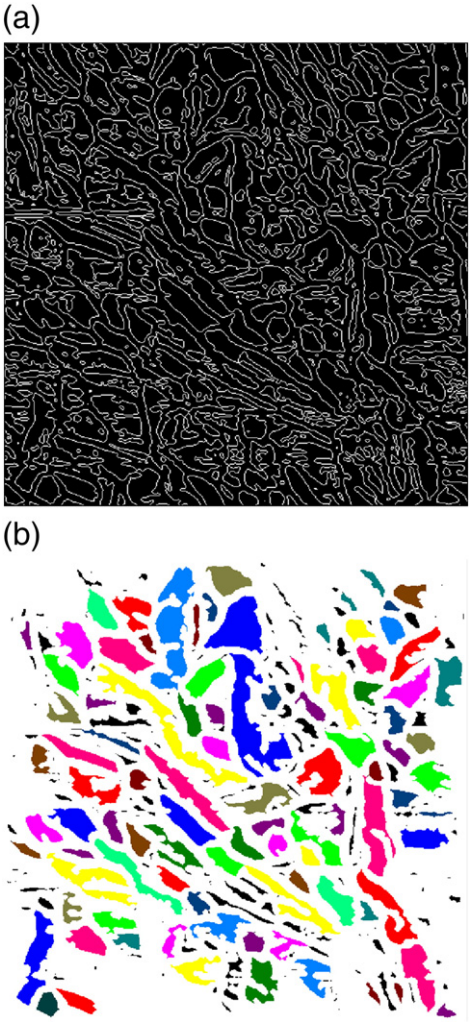

Fig. 15 – Results of applying edge detection technique to pentacene film on mica sample shown in Fig. 4b. (a) Detected edges of the mica sample. (b) Detected structures of the mica sample.

upon further inspection it is apparent that it has erroneously classified the areas between structures as structures.

After several iterations, the results shown in Fig. 14c can be obtained. The detected structures map well to the structures in the unprocessed AFM data and are comparable to the results obtained by the enhanced fuzzy logic. The main drawback of the watershed is that it requires a lot of manual fine tuning to obtain the desired results.

4.3. *Edge Detection Results*

Zero-crossing or Laplacian are the methods best suited to edge detection for detecting structure boundaries. Thus they can be employed to yield closed loop contours of images. These contours will be the boundaries of the detected structures.

The pentacene on mica sample is examined using these edge detection techniques. The intermediate structural contours are shown in Fig. 15a while the final results are shown in Fig. 15b. Although it has been possible to capture the main structures of the sample using this method, a large number of false small structures appeared in the results. Moreover, most of the structures at the edges of the film have been missed.

5. Conclusion

In this work we have presented a fuzzy logic based analysis technique capable of automatically characterizing AFM images. The technique can be applied to different surfaces regardless of how crowded the features of interest are. The technique employs an enhanced search-and-associate mechanism that resolves even intricate structure boundaries. A case study is also presented in which the fuzzy logic technique was used to extract quantitative information about two specimens, each having a different particle size distribution. The technique was able to capture these differences automatically. Our results show that the Enhanced Fuzzy logic technique provides a reliable method to extract quantitative structural information from AFM images without the need for manual adjustment of algorithm parameters.

REFERENCES

[1] Low T, Li MF, Fan WJ, Ng ST, Yeo Y-C, Zhu C, et al. Impact of surface roughness on silicon and germanium ultra-thin-body MOSFETs. Proc IEEE Int Elect Dev Meet December 13–15; 2004. p. 151–4.
[2] Nathan A, Park B, Sazonov A, Murthy RVR. Roughness of TFT gate metallization and its impact on leakage, threshold voltage shift and mobility. Mater Res Soc Symp Proc April 24–28 2000; A28.6.
[3] da Silva Jr JB, de Vasconcelosa EA, dos Santosa BECA, Freireb JAK, Freireb VN, Fariasb GA, et al. Statistical analysis of topographic images of nanoporous silicon and model surfaces. Microelectron J 2005;36:1011–5.
[4] Zhao Y, Wang G-C, Lu T-M. Characterization of Amorphous and Crystalline Rough Surfaces: Principles and Applications. 1st Edition. San Diego: Academic Press; 2001.
[5] http://www.pacificnano.com/.
[6] Bertrand G. On topological watersheds. J Math Imaging Vision 2005;22(2–3):217–30.
[7] Bertrand G. Some properties of topological greyscale watersheds. Procs SPIE Vision Geometry XII, 5300; 2004. p. 182–91.
[8] Al-Mousa A, Niemann DL, Gunther NG, Rahman M. Systematic quantitative characterization of surface nanostructures by scanning probe microscopy of thin-films. J Exp Nanosci, doi:10.1080/17458080903531039.
[9] Al-Mousa A, Niemann DL, Gunther NG, Rahman M. Systematic quantitative characterization of surface nanostructures. NanoTech Conf Proc May 2009;1 Chapter 4. Houston.
[10] Al-mousa A, Niemann DL, Gunther NG, Rahman M. A crystal recognition methodology for systematic quantitative characterization of nano-scale crystals. Mater Res Soc Symp March 24–28 2008;V8.17.
[11] Timothy Ross. Fuzzy Logic with Engineering Applications. 2nd Edition. Wiley; 2004.
[12] Nedeljkovic I. Image Classification Based on Fuzzy Logic. Comm. VI, ISPRS Congress, Istanbul; 2004.
[13] Karnowski Thomas P, Gleason Shaun S, Tobin Jr Kenneth W. Fuzzy logic connectivity in semiconductor defect clustering. Proc SPIE Int Soc Opt Eng 1998;3306:44.